of a ligamentous injury on cartilage mechanical properties using 3D indentation mapping.

Methods: Five 14-weeks old Lewis rats were used in this study and housed at the INRS-LNBE animal facility following Canadian guidelines for animal care and experimentation. Their hindlimb joints were assigned to three different groups (Control, Rupture and Contralateral). For one animal, both joints were left uninjured and used as Control (n=2). The remaining four animals were subjected to the non-invasive ACL rupture using an adapted mechanical loading protocol with a custom fixture and testing system (Mach-1v500cs, *Biomomentum*). Only their right hindlimbs were subjected to the ACL rupture (n=4 part of the Rupture group), while their left hindlimbs were left uninjured (n=4 part of the Contralateral group). On the day of injury, the right knee of anesthetized animals was flexed on a bottom platen while the paw was maintained in a top platen. The hindlimb was then subjected to a preconditioning followed by a rapid vertical displacement of 2 mm at 8 mm/s. This rapid loading caused an anterior subluxation of the tibia over the distal femur which results in ACL failure. Euthanasia of animals was performed 4 weeks post-injury; Femoral distal ends and tibial plateaux were collected (n=20 with 10 tibial plateaus and 10 femoral condyles) and cartilage was assessed mechanically by indentation and thickness mapping using a mechanical tester (Mach-1v500css, *Biomomentum*). Mapping grids were defined for each surface and normal indentation mapping was performed at each position based on the surface orientation (amplitude=0.05mm at 0.05mm/s). The resulting force was measured with a spherical indenter (r=0.5mm) fixed onto a multiaxial loadcell (17N). The spherical indenter was then replaced with a needle probe and moved towards the surface at each position of the same grid. Cartilage thickness was estimated using the displacement between the initial contact force and the sudden force increase when the needle tip transitions from the softer cartilage to the stiffer bone. The Instantaneous Modulus at each position was obtained by fitting the load-displacement curve to an elastic model in indentation using the measured thickness.

Results: Animal health technicians noted that animals were walking on tiptoes for a few days following injury. At necropsy, ACL rupture was confirmed on the right knee of all injured animals while an intact ACL was observed on their left hindlimbs as well as both hindlimbs of the control animal. Instantaneous modulus and cartilage thickness mappings of the femoral condyles and tibial plateaus were generated for all groups (Fig. 1).

The cartilage thickness measured for control samples were in line with the literature. In comparison, the cartilage was thicker in the entire femoral condyles in the Rupture group suggesting cartilage swelling (Fig. 2A). On the other hand, only the medial and lateral posterior regions of the contralateral femoral condyles showed an increase in thickness (Fig. 2A). The cartilage thickness in tibial plateaus did not show any significant difference between all groups (Fig. 2B). The medial-anterior regions of the femoral condyles and the tibial plateaus of the Rupture group have a significant decline in their mechanical properties (Fig. 2C&D). Similarly, the medial-anterior region of the tibial plateau also showed a significant decrease in instantaneous modulus in the Contralateral group (Fig. 2D).

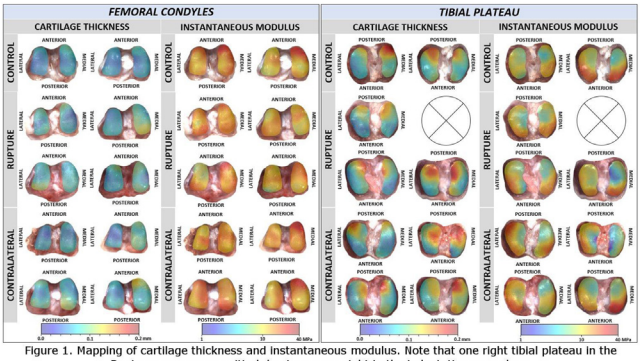

Figure 1. Mapping of cartilage thickness and instantaneous modulus. Note that one right tibial plateau in the Rupture group was omitted due to an oversight in the indentation procedure.

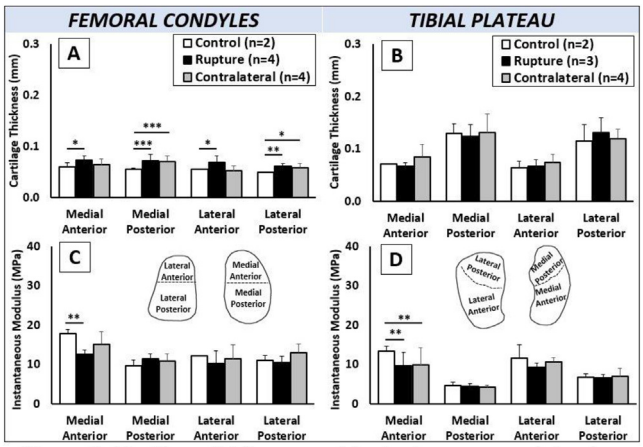

Figure 2. Cartilage thickness and instantaneous modulus bar graphs for different regions of rat femoral condyles and tibial plateaus in all groups. * p<0.05; ** p<0.01; *** p<0.001.

Conclusions: The Mach-1 system was successfully used to induce a non-invasive ACL rupture and mechanically characterize early post-traumatic cartilage degeneration through a unique 3D indentation and thickness mapping technique. Results show significant differences between the Control and Rupture group related to cartilage swelling and a decrease in instantaneous modulus in the medial anterior regions of both femoral and tibial knee surfaces.

300

DECIPHERING UROLITHINS A AND B ACTIVITIES ON MUSCLE: TRANSCRIPTOMIC MODULATION ON HUMAN PRIMARY MYOTUBES

Y. Henrotin, C. Lambert, A. Florin, J. Zappia, P. Centonze, C. Sanchez. *Univ. of Liège, Liège, Belgium*

Purpose: Urolithins are intestinal bacterial metabolites of ellagic acid, from pomegranate and nuts. They modulate oxidative-regulated pathways and display anti-inflammatory, antioxidative properties. Several studies indicate that they could be inducers of muscle strengthening. The aim of this in vitro study was to investigate their mechanisms of action at plasma concentrations on primary human myotubes.

Methods: Urolithin A and B (UA and UB, 1-10 μg/mL) were evaluated separately on primary human muscle CD56+ cells, isolated from the vastus lateralis of 6 men and 3 women (aged range 55 to 96-y) and differentiated in myotubes. 24h-treatment mRNA-sequencing of these 9 patients was studied by DESeq2 analysis (R software). Modulation of several target genes was then validated by RT-qPCR on 4 patients.

Results: After 24h of treatment at 5 μM, UA and UB significantly modified the expression of 1779 and 319 genes, respectively (adjusted p-value of 0.01 and Log2FoldChange |>0.32|). Among the most regulated genes, we found genes involved in myoblasts to myotubes differentiation. UA increased the expression of NOTCH1 (+73%), MYMX (+70%), PANX1 (+50%), MSTN (+64%) and conversely decreased FGF9 (-75%), MRLN (-33%) and ICAM5 (-52%). Regarding UB, it decreased IGFN1 (-75%), TGFBI (-60%), STC2 (-35%) and increased TGM2 (+59%). We also have observed the modulation of genes involved in the inflammatory process. Thus, LIF was increased by 80% by UA and PTGS1 was decreased by 41% by UA and by 43% by UB. UA and UB had the opposite effect on IL17B, a cytokine involved in tissue repair but its role in muscle is still to be defined. IL17B was decreased by 49% by UA and conversely upregulated by 45% by UB. Finally, we confirmed the modulation of NOTCH1, MYMX, FGF9, ICAM5, STC2, PTGS1, and IL17B following UA and UB treatment at 1, 5 and 10 μM by RT-qPCR.

Conclusions: At plasma concentrations, UA seems more active than UB. It promotes the differentiation process of myoblasts to myotubes. In parallel, urolithins present anti-inflammatory properties, mainly by reducing the PGE2 synthesis via PTGS1, but also for UA by increasing LIF. Our data provide a better understanding of urolithin activities and highlight the importance of the gut microbiome in muscle health.